# In vitro evaluation of pH-sensitive cholesterol-containing stable polymeric micelles for delivery of camptothecin

Partha Laskar [a], Sintu Samanta [b], Sudip Kumar Ghosh [b,*], Joykrishna Dey [a,*]

[a] Department of Chemistry, Indian Institute of Technology, Kharagpur 721 302, India
[b] Department of Biotechnology, Indian Institute of Technology, Kharagpur 721 302, India

## ABSTRACT

Two novel amphiphilic statistical copolymers poly(cholesteryl acrylate-co-methoxypoly(ethylene glycol) methacrylate), poly[$CHOL_y$-co-$mPEG_{n,x}$] (for $n = 5$, $x = 110$ and $y = 15$, and for $n = 23$, $x = 22$ and $y = 3$) with copolymer composition ($x:y$) of 7:1 were designed and synthesized as a delivery system for water-insoluble anticancer agent, S-(+)-camptothecin (CPT). The polymers were synthesized using reversible addition fragmentation chain transfer (RAFT) polymerization technique and they were found to form stable polymeric micelles in water above a relatively low critical concentration. The polymeric micelles (PMs) were characterized by a number of techniques including surface tension, fluorescence, dynamic light scattering, and electron microscopy. Incorporation of CPT into the micelles and the stability of CPT-loaded micelles were studied by spectrophotometric method. Sustained release of an encapsulated fluorescent guest triggered by hydrolysis of the ester linkages in acidic pH is demonstrated. The polymers are not only hemocompatible and nontoxic in the allowed concentration range, but also they can easily permeate into the cancer cells (MCF7 and HeLa). The in vitro drug delivery assay of CPT-loaded polymeric micelles on cancer cells (HeLa) showed very good chemotherapeutic activity in the biocompatible concentration range of the copolymers.

## 1. Introduction

Camptothecin (CPT, Chart 1(a)), a naturally occurring alkaloid, is a potent chemotherapeutic drug for different types of cancer. Structure–activity studies have shown that the closed lactone ring and the C-20-OH group in CPT are critical for its anticancer activity [1,2]. However, poor aqueous solubility (2.5 μg/mL) [3] and chemical instability due to hydrolysis (see Chart 1(a)) of the lactone ring under physiological condition limit its application. To overcome this, different strategies were adopted by researchers [4–27]. First, a number of water-soluble analogs, such as topotecan and irinotecan (CPT-11) were synthesized, but most of them were found to be less potent than the parent drug [4–6]. However, it has been shown that acylation of the 20-OH group significantly increases stability of the lactone ring [7,8]. Thus the second approach that has gained a huge attention in the recent literature is to convert the drug into an inactive but more stable prodrug that reverts back to the pharmacologically active agent triggered by biological stimuli.

Greenwald et al. are the first to use the prodrug approach which utilizes the 20-OH group of CPT to condense with a 40 kDa PEG

dicarboxylic acid [9]. They achieved increased circulatory retention as well as continuous therapeutic release of CPT. Subsequently, CPT was conjugated with many water-soluble polymers, such as poly(ethylene glycol) (PEG) [6], poly[N-(2-hydroxypropyl) methacrylamide] [10] and poly(L-glutamic acid) [11] through acylation of the 20-OH group and the resulting polymer-CPT conjugates were evaluated as antitumor polymer prodrugs. Yurkovetskiy et al. conjugated CPT with a 60 kDa biodegradable hydrophilic polyacetal and demonstrated its increased half-life (~14.2 h) in the blood [12]. These polymer-CPT conjugates showed improved drug pharmacokinetics and resulted in an increased accumulation of CPT in tumors by "enhanced permeation and retention" (EPR) effect [13]. To enhance chemical stability and long-term circulation of CPT, Liu's group synthesized mPEGylated α,β-poly(L-aspartic acid]-CPT conjugates to fabricate nanomicelles [14]. Recently, Fan et al. have developed a nanomicelle based on α,β-poly(N-carboxybutyl)-L-aspartamide]-CPT and achieved increased solubility and stability of CPT [15]. Shen and coworkers by taking advantage of the extreme hydrophobicity of CPT, conjugated CPT to a very short oligoethylene glycol (OEG) chain producing amphiphilic prodrug, OEG–CPT that formed liposome-like nanocapsules in water with a CPT content as high as 58 wt% [16]. Lee et al. synthesized oxidative stimuli-responsive nanoprodrug of CPT by linking it to

\* Corresponding authors. Fax: +91 3222 255303 (J. Dey).
*E-mail address:* joydey@chem.iitkgp.ernet.in (J. Dey).

tetraethylene glycol via a carbonate bond [17]. More recently, Li's group designed a novel PEG–CPT prodrug that spontaneously formed nanomicelles which released the cytotoxic drug under tumor-relevant reductive conditions [18]. An alternative strategy would be to develop suitable carriers that can solubilize as well as protect CPT from hydrolysis. In fact, many reports have shown that the lactone ring of CPT can be protected upon incorporation into a lipid bilayer structure, such as liposomes [19], microspheres [20,21] or nanohybrids [22]. Several systems based on lipid nanoparticles [23,24], dendrimers [25], solid lipid nanoparticles [26], and nanoemulsions [27] were also devised to better deliver CPT.

On the other hand, polymeric micelles (PMs) usually prepared from amphiphilic block copolymers have also received much attention in drug delivery research and have been applied to anticancer drugs such as doxorubicin [28], paclitaxel [29,30], cisplatin [31], and methotrexate [32]. In 2012, Yang and coworkers have reported the delivery of paclitaxel using a series of cholesterol-containing biodegradable block copolymers [30]. Also in 2013, several groups reported self-assembly formation by cholesterol-conjugated copolymers for drug delivery application [33]. Usually PMs in the size range of 40–200 nm reduces renal clearance and scavenging by the reticuloendothelial system (RES) and exhibit EPR effects at solid tumor sites for passive targeting [34]. Maitani and coworkers have successfully employed poly(ethylene glycol)-poly(L-aspartate ester) block copolymer micelles for CPT with high incorporation efficiency [35–37]. However, except a couple of reports [38] from this group, there are no reports on solubilization of CPT by amphiphilic statistical copolymer micelles. In our earlier report, we have demonstrated spontaneous and stable micelle formation by a series of random polymers having different amount of same fatty acid chain as hydrophobe [39]. These PMs were observed to enhance aqueous solubility as well as protect CPT from hydrolytic degradation [39]. Further, 14–15% hydrophobe content in the polymeric backbone was found to be suitable for in vitro drug delivery [39]. This report actually encouraged us to investigate the possible polymeric self-assembly formation using cholesterol (CHOL) as hydrophobe instead of fatty acid as a better drug delivery system (DDS). CHOL being more lipophilic than the hydrocarbon chain of a fatty acid the PMs produced by the copolymer are expected to greatly enhance the solubility of CPT. Also cholesterol is an important component of animal cellular membrane and responsible for membrane fluidity and permeability, intracellular transport, signal transduction, and cell trafficking [40–44]. Since cholesterol is associated with so many membrane-related bioprocess, so incorporation of cholesterol may be helpful for any DDS to cross the cellular membrane more easily. Therefore, in the present study, we have synthesized two amphiphilic copolymers, poly (cholesteryl acrylate-co-methoxypoly(ethylene glycol) methacrylate), poly[CHOL$_y$-co-mPEG$_{n,x}$] (for $n = 5$, $x = 110$ and $y = 15$, and for $n = 23$, $x = 22$ and $y = 3$) with copolymer composition ($x$:$y$) of 7:1 (Chart 1(b)) with CHOL as hydrophobe unit and mPEG$_n$ as hydrophilic group. Because of the presence of CHOL these amphiphilic statistical copolymers are expected to have a strong tendency to form micelles with a very low critical aggregation concentration (CAC) [45]. The PMs formed by these copolymers will have a hydrophobic core made of CHOL within which hydrophobic drugs can be entrapped and a hydrophilic shell of PEG chains. PEG was chosen for the hydrophilic segments because of its (i) good water solubility, (ii) biocompatibility, and (iii) reduced uptake by the RES [46–48]. These will result in a prolonged circulation half-life in the bloodstream in comparison to nonPEG coated carriers. These copolymers were characterized by a number of techniques, including surface tension, light scattering, fluorescence, and electron microscopy. They were investigated to determine their potential application in the encapsulation and hydrolysis-triggered delivery of the chemotherapeutic drug CPT.

## 2. Results and discussion

### 2.1. Synthesis and molecular characterization

For the synthesis of copolymers, cholesteryl acrylate (CHOL) monomer was first synthesized according to literature reported method [49]. The statistical copolymers poly[CHOL$_y$-co-mPEG$_{5,x}$] and poly[CHOL$_y$-co-mPEG$_{23,x}$] were then synthesized from CHOL and methoxypoly(ethylene glycol) methacrylate (mPEG$_n$, $n = 5$ and 23) by reversible addition–fragmentation chain transfer (RAFT) polymerization technique. The details of synthesis and chemical identification are given under "Supporting Information" (SI). The $^1$H and $^{13}$C NMR spectra confirmed the chemical structure of the CHOL monomer (Figs. S1 and S2; SI) and the copolymers (Figs. S3 and S4; SI). The average molecular weight ($M_w$) and polydispersity ($D$) of poly[CHOL$_y$-co-mPEG$_{5,x}$] (39 kDa; $D = 1.44$) and poly[CHOL$_y$-co-mPEG$_{23,x}$] (25 kDa; $D = 1.26$) copolymers were obtained from conventional GPC technique using polystyrene as standard. The copolymer ratio was calculated from the $^1$H NMR spectra (Figs. S3 and S4; SI) using chemical shift positions of –OCH$_3$ group ($\sim\delta$ 3.3 ppm) of PEG chain and –CH$_3$ group ($\sim\delta$ 0.6 ppm) of CHOL. The copolymer ratio for both the polymers was found to be 1:7, which means about 12% (mol) of CHOL is present in the polymer. From these data we calculated the number of CHOL ($y$) and mPEG$_n$ ($x$) monomer units in the polymer chain. The $x$ and $y$ values thus obtained are respectively, 15 and 110 for poly[CHOL$_y$-co-mPEG$_{5,x}$] copolymer and 3 and 22 for poly[CHOL$_y$-co-mPEG$_{23,x}$] copolymers. This means that the degrees of polymerization are different for the copolymers. The molecular formula of the copolymers can thus be represented as poly[CHOL$_{15}$-co-mPEG$_{5,110}$] and poly[CHOL$_3$-co-mPEG$_{23,22}$].

### 2.2. Self-assembly studies

The reduction of surface tension of water (Fig. S5; SI) with increasing polymer concentration ($C_p$) suggests that the statistical copolymers are amphiphilic in nature. Of the two copolymers, poly[CHOL$_{15}$-co-mPEG$_{5,110}$] showed greater surface activity than poly[CHOL$_3$-co-mPEG$_{23,22}$] as indicated by the $\gamma_{min}$ values. This can be attributed to higher polarity of the latter copolymer with long mPEG$_n$ chain. Despite similar copolymer composition the latter copolymer has CHOL content less and mPEG chain length longer than that of the former, which reduces surface adsorption of the copolymer. Since the $\gamma$-value decreased over a large concentration range and there was no sharp break in the surface tension plot, it was difficult to determine CAC.

Therefore, steady-state fluorescence of NPN was measured at different polymer concentrations in order to study self-assembly behavior. Basically NPN is weakly fluorescent in water and shows a $\lambda_{max}$ around 455 nm. When it is being solubilized in nonpolar medium or hydrophobic core of the micelles or any other aggregates, the fluorescence spectrum of NPN exhibits a large blue shift in addition to intensity rise indicating formation of the micelles/aggregates with a hydrophobic core containing the probe molecules [38b]. We observed a $\sim$40 nm (Fig. 1a) blue shift of $\lambda_{max}$ with a 8–10-fold intensity rise (Fig. S6) for NPN fluorescence in presence of both the polymers. To determine the CAC value of the copolymers, the spectral shift $\Delta\lambda$ ($=\lambda_{max(water)} - \lambda_{max(polymer)}$) of NPN was plotted against $C_p$. The plots in Fig. 1a depicts that $\Delta\lambda$ is very low and independent of $C_p$ in dilute solutions, but they exhibit a sharp rise above a critical concentration. This observation suggests that the aggregation started above this critical concentration through the inter-chain aggregation. The CAC values as obtained from the onset of rise of $\Delta\lambda$ value are $1.73 \times 10^{-4}$% (1.73 µg/mL) and $8.26 \times 10^{-4}$% (8.26 µg/mL) for poly[CHOL$_{15}$-co-mPEG$_{5,110}$] and
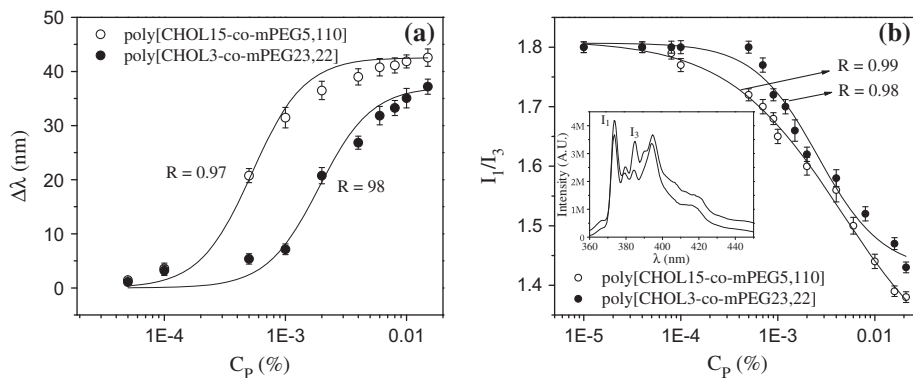
**Fig. 1.** (a) Plot of shift of emission maximum [$\Delta\lambda = \lambda_{max(water)} - \lambda_{max(polymer)}$] of NPN probe as a function of copolymer concentrations ($C_p$ %, w/v). (b) Plot of fluorescence intensity ratio ($I_1/I_3$) of Py versus copolymer concentration ($C_p$, %, w/v). Inset: Fluorescence emission spectra of Py showing $I_1$ and $I_3$ bands in water and in the presence of 0.01% (w/v) poly[CHOL$_{15}$-co-mPEG$_{5,110}$].

poly[CHOL$_3$-co-mPEG$_{23,22}$], respectively. In addition to that of NPN study, steady-state fluorescence of pyrene (Py) was also measured at different polymer concentrations in order to reestablish the self-assembly behavior. The intensity ratio ($I_1/I_3$) of the first (372 nm) and the third (384 nm) vibronic peak of the fluorescence emission spectrum of Py is known to be sensitive to the polarity of the medium [50,51]. The variation of $I_1/I_3$ as a function of $C_p$ is shown in Fig. 1b. At low concentrations of the polymers, the $I_1/I_3$ values were observed to be close to the value in water (1.8), which then decreased following a sigmoid curve with further increase of $C_p$, suggesting partitioning of Py into the hydrophobic domains. The feature of the titration curves clearly indicates that the copolymers form micelles through inter-chain association. The CAC values as obtained from the onset of fall of $I_1/I_3$ value are $1.81 \times 10^{-4}\%$ (1.81 µg/mL) and $8.42 \times 10^{-4}\%$ (8.42 µg/mL) for poly[CHOL$_{15}$-co-mPEG$_{5,110}$] and poly[CHOL$_3$-co-mPEG$_{23,22}$], respectively. These values are closely similar to those obtained from the fluorescence titration using NPN probe and thus confirm accuracy of the methods. However, since fluorescence properties of NPN are more sensitive to change of polymer concentration, the CAC values obtained from fluorescence titration using NPN can be taken as more accurate. The low $I_1/I_3$ value (1.40) of Py in both 0.1% copolymer solutions clearly indicates that the probe molecules are solubilized within microdomains having polarity equivalent to ethyl acetate ($I_1/I_3$ = 1.45) solvent [51].

On the other hand, the steady-state fluorescence anisotropy ($r$) value of 1,6-diphenyl-1,3,5-hexatriene (DPH) probe measured in the presence of 0.1% poly[CHOL$_{15}$-co-mPEG$_{5,110}$] (0.290) or poly[CHOL$_3$-co-mPEG$_{23,22}$] (0.244) suggests that the microenvironment of the PMs is very viscous [52]. The microviscosity ($\eta_m$) values were estimated according to the procedure described by Dey and coworkers [53]. The $\eta_m$ values thus obtained from fluorescence anisotropy ($r$) and lifetime ($\tau_f$) data (Table S1; SI) of the DPH probe using Stokes–Einstein–Debye (SED) equation [54] for the micelles of poly[CHOL$_{15}$-co-mPEG$_{5,110}$] (333 mPa s) and poly[CHOL$_3$-co-mPEG$_{23,22}$] (149 mPa s) are very high compared to that of normal surfactant micelles of Triton-X100 (39.81 mPa s) [53].

The transmission electron microscopic (TEM) images of the polymer solutions were taken at a concentration above their CAC values. The micrographs in Fig. 2(a and b) clearly reveal the spherical particles of diameter around 20 nm for poly[CHOL$_{15}$-co-mPEG$_{5,110}$], and around 60 nm for poly[CHOL$_3$-co-mPEG$_{23,22}$] copolymers. It is important to note that the PMs have reasonably narrow size distributions. The hydrodynamic diameters ($d_h$) of the PMs were also measured directly by dynamic light scattering (DLS) technique. The size distributions of the PMs formed by the copolymers are shown in Fig. 2(c and d). As seen the mean hydrodynamic diameters of the micelles of poly[CHOL$_{15}$-co-mPEG$_{5,110}$]

(ca. 20–25 nm) and poly[CHOL$_3$-co-mPEG$_{23,22}$] (ca. 65–70 nm) are closely equal to the corresponding value obtained from TEM measurements. However, the $d_h$ value of the PMs of poly[CHOL$_{15}$-co-mPEG$_{5,110}$] is much less than that of poly[CHOL$_3$-co-mPEG$_{23,22}$]. Since the latter copolymer is more polar due to its low molecular weight and longer mPEG$_n$ chains, the PMs formed are less compact compared to those of former copolymer. This might cause fusion of the PMs forming larger micelles.

### 2.3. Thermal stability of the PMs

The physical stability of the PMs in aqueous media is important parameter in drug delivery. They should be stable at the physiological condition (pH 7.4, 37 °C). It should be noted that aqueous solutions (pH 7.4) of both copolymers (0.1%) exhibit cloudiness above a critical temperature. This is shown by the transmittance (%T) versus temperature plots in Fig. 3a. As observed the percent transmittance falls sharply to zero at a critical temperature which can be taken as a phase transition temperature. The cloud point temperatures of poly[CHOL$_{15}$-co-mPEG$_{5,110}$] and poly[CHOL$_3$-co-mPEG$_{23,22}$] are 330 K (57 °C) and 338 K (65 °C), respectively. As reported for other PEG-containing copolymers, this is due to temperature-induced dehydration of the PEG chains which makes polymer chain more hydrophobic [55,56]. The slightly higher value of the cloud point and hence higher stability in the case of poly[CHOL$_3$-co-mPEG$_{23,22}$] is due to its longer mPEG$_n$ chains that interact with the mPEG$_n$ chains of other micelles.

The thermal stability of the PMs was further studied by fluorescence probe method using DPH as a probe molecule. Since the polymer solutions exhibit cloud point above 330 K (55 °C), the fluorescence spectra of DPH were measured at different temperatures in the range 293–328 K (20–55 °C) in pure water as well as in the presence of the copolymers. As can be seen in Fig. 3b, the fluorescence intensity of the entrapped DPH molecules in 0.1% aqueous copolymer solution decreases gradually with the increase of temperature. Also, as observed from the plots in Fig. S7 (SI), the $r$-value of DPH probe decreases in this temperature range, indicating increase of internal fluidity of the micelles. The control experiment in pure water, however, did not show any significant change (Fig. 3b, inset). We also measured hydrodynamic size of the micelles at 310 K (37 °C). The size distributions of micelles as shown in Fig. S8 (SI), exhibit a very small shift toward larger $d_h$ values, suggesting good thermal stability of the PMs at the physiological temperature. This decrease of DPH fluorescence with rise in temperature is due to increased fluidity as well as the loss of hydrophobicity of the micellar core at higher temperatures which results in a reduction of the partition coefficient of DPH molecule.
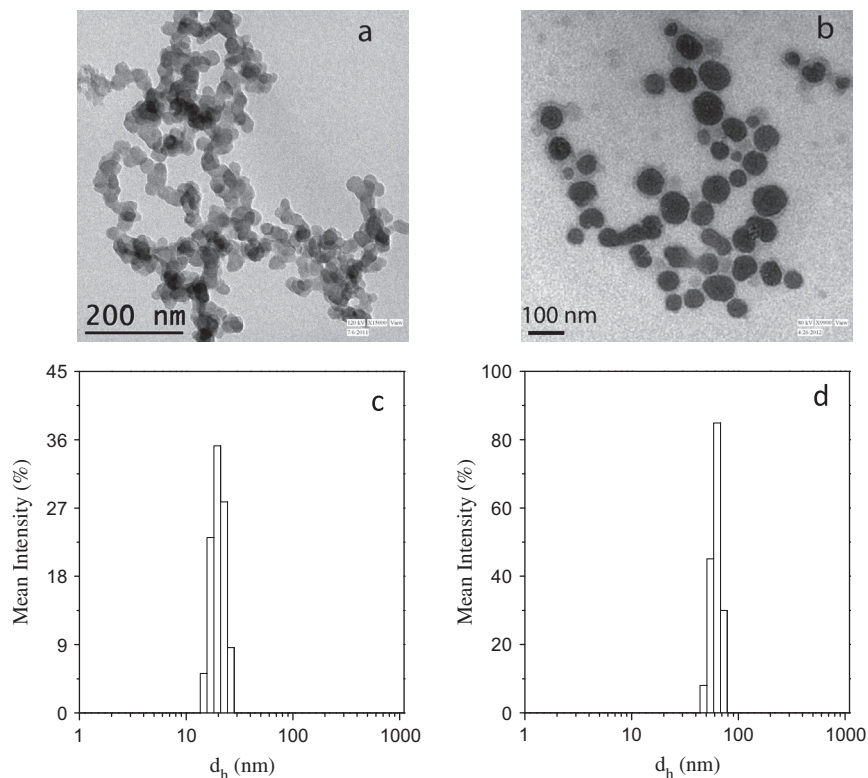
**Fig. 2.** TEM images of PMs in 0.1% (w/v) aqueous solutions of (a) poly[CHOL$_{15}$-co-mPEG$_{5,110}$], and (b) poly[CHOL$_3$-co-mPEG$_{23,22}$] at 298 K; hydrodynamic size distribution profiles of the aggregates in 0.1% (w/v) aqueous copolymer solutions of (c) poly[CHOL$_{15}$-co-mPEG$_{5,110}$] and (d) poly[CHOL$_3$-co-mPEG$_{23,22}$] at 298 K.
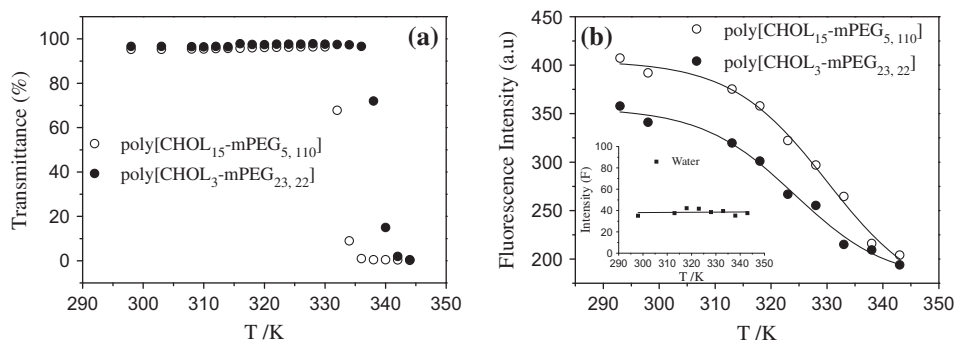


**Fig. 3.** (a) Plot of percent transmittance (% T at $\lambda$ = 400 nm) of copolymer solutions (0.1%, w/v) as a function of temperature ($T$/K). (b) Variation of fluorescence intensity of DPH at $\lambda$ = 430 nm in aqueous copolymer solutions ($C_p$ = 0.1%, w/v) with temperature ($T$/K). Inset: plot of fluorescence intensity of DPH in water (pH 7) versus temperature ($T$/K).
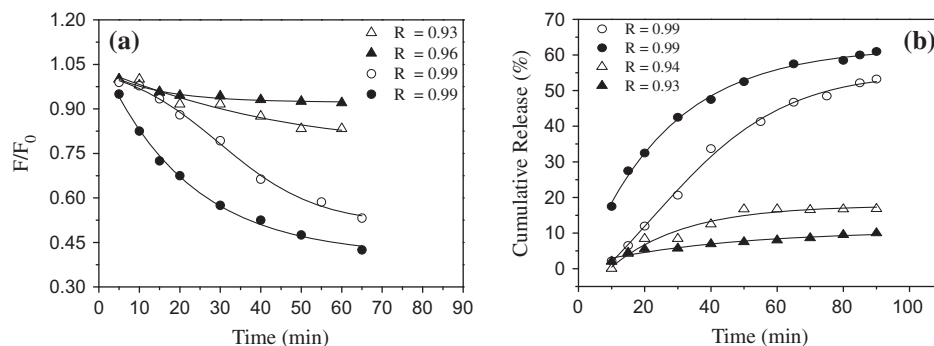


**Fig. 4.** Variations of (a) relative fluorescence intensity ($F/F_o$) of DPH at $\lambda$ = 430 nm and (b) cumulative (%) release of DPH with time in aqueous solutions ($C_p$ = 0.1%, w/v) at 310 K for (○) poly[CHOL$_{15}$-co-mPEG$_{5,110}$], and (●) poly[CHOL$_3$-co-mPEG$_{23,22}$] at pH 4.7, and for (▲) poly[CHOL$_{15}$-co-mPEG$_{5,110}$] and (△) poly[CHOL$_3$-co-mPEG$_{23,22}$] at pH 7.4.
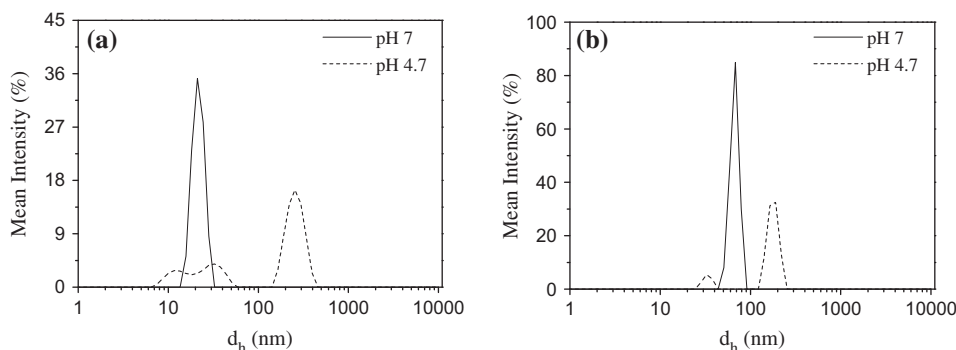
**Fig. 5.** Hydrodynamic size distributions of the PMs of (a) poly[CHOL$_{15}$-co-mPEG$_{5,110}$] and (b) poly[CHOL$_3$-co-mPEG$_{23,22}$] copolymers (0.1%) in neutral (20 mM, pH 7.0) and in acidic (20 mM, pH 4.7) buffer after 2 h of incubation period at 298 K.

## 2.4. Hydrolysis-triggered drug release

As mentioned earlier, both CHOL and PEG chains are connected to the polymer backbone through ester linkages. Therefore, they can be easily hydrolyzed in either acidic or basic aqueous medium. Because drug molecules are incorporated only by physical entrapment within the PMs, they can be easily released from the hydrophobic core in acidic condition. The hydrolysis (or drug release) kinetics of the PMs was studied in both biological pH (7.4) and acidic pH (4.7, typical of tumor cells) conditions using DPH as a model drug. The fluorescence intensity change of DPH was monitored as a function of time at the physiological temperature (310 K). The variation of relative fluorescence intensity ($F/F_o$, where $F_o$ and $F$ are the intensities before and after the start of the hydrolysis reaction, respectively) of the DPH probe with time at pH 7.4 and 4.7 are shown in Fig. 4(a). It is observed that at the biological pH, DPH fluorescence does not change significantly with time, suggesting that the PMs are quite stable in this pH. This is further supported by the fact that the size distribution (Fig. S9, SI) of the PMs also does not change significantly even after incubation of the solution for 6 h. In contrast, at pH 4.7, the fluorescence intensity of the DPH decreased with time for both copolymers following first-order decay. The corresponding plots showing variation of percentage of DPH released with time are also depicted in Fig. 4(b). The DLS measurements also showed a corresponding change in size distribution (Fig. 5) after 2 h of incubation period. The appearance of a new distribution profile corresponding to aggregates of larger diameters in the case of both polymers can be observed. This is due to the hydrolytic degradation of the hydrophobic part from the polymeric backbone at the acidic pH which results in the formation of less compact bigger size aggregates. This clearly indicates a gradual release of DPH molecules from the hydrophobic microdomains of
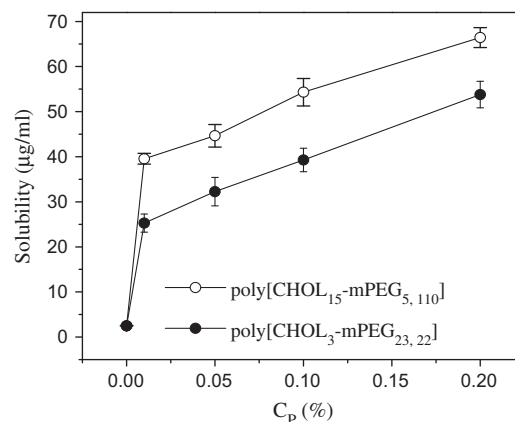


**Fig. 6.** Variation of solubility (μg/mL) of CPT with copolymer concentration ($C_p$) in phosphate buffer (20 mM, pH 7.4) at 298 K.

the PMs as a result of hydrolysis of the ester bonds in the side chains. In order to obtain the rate constant of the DPH release, the fluorescence intensity profiles were fit to first-order decay equation. It is observed that with poly[CHOL$_3$-co-mPEG$_{23,22}$] the release rate ($k = 1.5 \times 10^{-2}$ min$^{-1}$) is slightly faster than that with poly[CHOL$_{15}$-co-mPEG$_{5,110}$] ($k = 0.9 \times 10^{-2}$ min$^{-1}$) polymer. The corresponding half-life of the drug release are ca. 46 min and 77 min for poly[CHOL$_3$-co-mPEG$_{23,22}$] and poly[CHOL$_{15}$-co-mPEG$_{5,110}$], respectively. This difference must be due to the relatively less rigid microenvironments of the micelles of the former copolymer. The results suggest that the structural instability of the copolymers can be used as a pH-triggered release of hydrophobic drug molecules in the cancer cells.
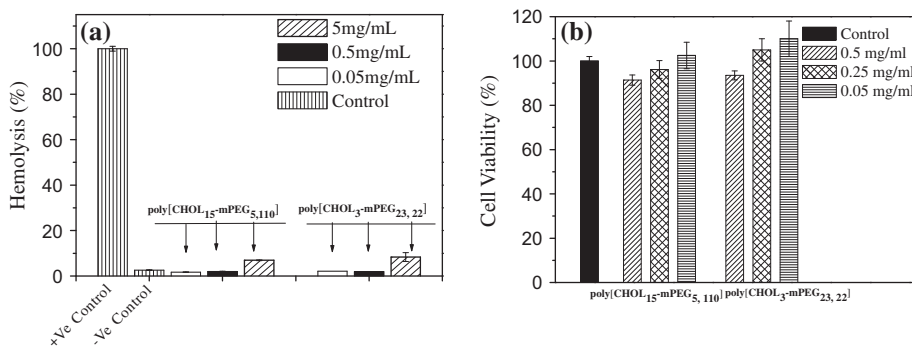


**Fig. 7.** (a) Hemolysis assay at different concentrations (0.05–5 mg/mL) of the copolymers at physiological pH (7.4). (b) Cytotoxicity effects of the polymers on HeLa cells. The cells were treated for 12 h with both the polymers at a concentration ranging from 0.05 to 0.5 mg/mL. Cell viability was measured by MTT assay and it was expressed as the percentage of growth with respect to untreated control cells. The data were presented as the mean ± SD.

## 2.5. Encapsulation of CPT

Encouraged by the results of fluorescence probe studies we investigated drug entrapment efficiency of the PMs formed by the copolymers. The solubility of the hydrophobic drug CPT in PBS buffer (1.33 μg/mL) [15] is very low, but it was observed to increase in the presence of copolymers due to their encapsulation within the hydrophobic micellar core. Plots in Fig. 6 show that the solubility increases linearly with the increase of polymer concentration above the CAC value of the copolymers. Both polymers showed a very high encapsulation efficiency for CPT. The amount of CPT loaded into the copolymer micelles is ca. 55 mg/g (or 5.5 wt%) for poly[CHOL$_{15}$-co-mPEG$_{5,110}$] and ca. 35 mg/g (or 3.5 wt%) for poly[CHOL$_3$-co-mPEG$_{23,22}$] copolymer. Thus the drug contents of these copolymers are better than polymer-drug conjugates, the drug contents in which is only a few percent to keep the conjugates water-soluble. For instance, the CPT content in its conjugate to a PEG with a molecular weight of 40 kDa was only 0.86–1.72% (w/w) [57,58]. It should be noted that although hydrodynamic size of the copolymer micelles of poly[CHOL$_3$-co-mPEG$_{23,22}$] is higher than those of poly[CHOL$_{15}$-co-mPEG$_{5,110}$], the latter showed higher drug loading capacity for CPT. The lower drug-loading capacity of the copolymer micelles of poly[CHOL$_3$-co-mPEG$_{23,22}$] must be due to its low CHOL content which results in the formation of relatively less compact and hence more polar micellar core which in turn reduces partitioning of CPT into the micelles.

It is important to note that CPT is solubilized within the PMs in its native closed lactone form. This is demonstrated by the measured fluorescence emission spectra of CPT in neutral (pH 7.0) and alkaline pH (12.0), and in the presence of polymer (Fig. S10; SI). It is observed that the fluorescence intensity of CPT in the carboxylate form (pH 12.0) is reduced and red-shifted with respect to the closed lactone form. One can also see that with the increase of $C_p$ the fluorescence intensity of CPT is decreased accompanied by a blue shift (Fig. S11; SI), indicating gradual partitioning of CPT from more polar bulk water to the hydrophobic microenvironment of the PMs [59]. The quenching of fluorescence with increasing $C_p$ value might be due to incorporation of more than one CPT molecules in each micelles which causes concentration quenching. This also explains greater solubilization capacity of the PMs employed in this work.

## 2.6. Hemocompatiblity studies

For intravenous drug delivery formulation, it is essential that the delivery system should be hemocompatible. Therefore, hemolytic assay was performed with Red Blood Cell (RBC) membranes in order to test the hemocompatibility of the copolymers. Percentage of hemolysis of RBCs with various concentration of copolymers (0.05–5 mg/mL) were compared with −ve control (RBC suspended in PBS) and +ve control (RBC suspended in 1% Triton X-100). Both the copolymers were found to be hemocompatible. Although hemolysis gradually increased with the polymer concentration, the polymers showed only 5–7% hemolysis at their highest concentration (5 mg/mL) (Fig. 7a). Thus these polymers can be considered as good carriers for intravenous drug delivery system. The low hemolytic behavior of these polymers must be due to the presence of low hydrophobic content and hydrophilic PEG groups on the surface of the polymeric micelles [60].

## 2.7. Cytotoxicity studies

To determine the cell viability of the polymers, HeLa (cervical cancer cell line) cells were cultured and treated with different concentrations (0.05–0.5%) of the polymers followed by the detection of the cytotoxicity using MTT assay. The percentages of viable HeLa

cells, relative to the untreated control cells were more than 90% when cultured for 12 h with 0.05, 0.25 and 0.5 mg/mL of poly[CHOL$_{15}$-co-mPEG$_{5,110}$]. Similar cell viability can also be observed with poly[CHOL$_3$-co-mPEG$_{23,22}$], with reference to the untreated control cells (Fig. 7b). At relatively higher concentrations, poly[CHOL$_{15}$-co-mPEG$_{5,110}$] showed less cell viability in comparison to poly[CHOL$_3$-co-mPEG$_{23,22}$] copolymer. This must be due to the longer PEG chain which makes the micelle surface more polar in the case of latter polymer. However, it should also be noted that due to the slightly higher molecular weight, poly[CHOL$_{15}$-co-mPEG$_{5,110}$] also has larger number of cholesterol unit per molecular chain in comparison to the poly[CHOL$_3$-co-mPEG$_{23,22}$]. The same
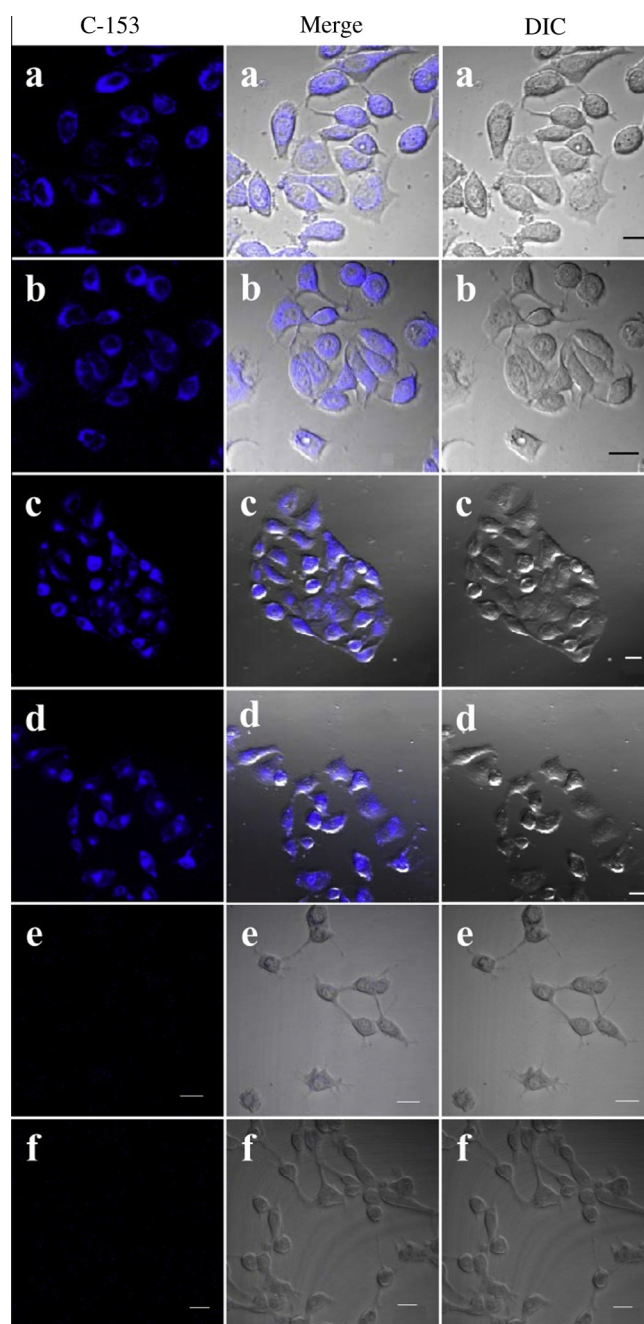


**Fig. 8.** Confocal microscopic images of MCF7 (a and b), HeLa (c and d) and L929 (e and f) cells incubated with C-153-loaded polymers (0.5 mg/mL): poly[CHOL$_{15}$-co-mPEG$_{5,110}$] (a, c, and e) and poly[CHOL$_3$-co-mPEG$_{23,22}$] (b, d, and f); the cells not treated with C-153 were taken as a negative control (data not shown); bar is 20 μm.
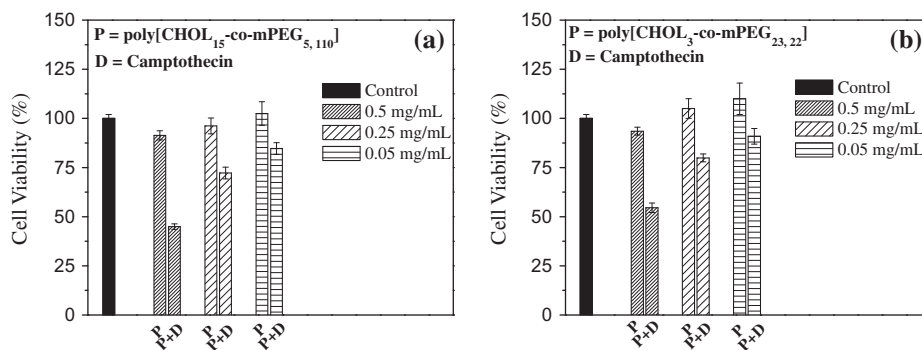
**Fig. 9.** Cytotoxicity effects of pure (a) poly[CHOL$_{15}$-co-mPEG$_{5,110}$] and (b) poly[CHOL$_3$-co-mPEG$_{23,22}$] polymers and CPT-loaded polymers (0.05 and 0.5 mg/mL) on HeLa cells. Cell viability was measured by MTT assay after 12 h of treatment and it was expressed as the percentage of growth with respect to untreated control cells. The data were presented as the mean ± SD.

pattern of the results was also observed in the cell viability study for around 24 h of incubation using MCF7 (breast cancer cell line) cells (Fig. S12, SI).

The analysis of confocal micrographs showed that a bright blue fluorescence was observed in the MCF7 (Fig. 8(a and b)) as well as HeLa (Fig. 8(c and d)) cells treated with coumarin 153 (C153) dye encapsulated polymers, while very low or no such fluorescence was observed for normal fibroblast cells (L929) (Fig. 8(e and f)). It indicates that both the MCF7 and HeLa (cervical cancer cell line) cells had shown the tendency to uptake more amount of both the copolymer micelles in their cellular compartment while the L929 cells did not show the same characteristics. Similar experiments were also performed with the CPT-loaded PMs of the copolymers under similar conditions. For in vitro evaluation of chemotherapeutic activity of the CPT-loaded micelles, the cell cytotoxicity of the copolymers was tested on HeLa cells [61]. The cells were incubated for 12 h at 310 K with different concentrations of CPT-loaded PMs in the media. Here, the PMs without any encapsulated drug were used as control. The copolymers were used at concentrations ranging from 0.05 to 0.5 mg/mL which have the least inhibitory effects on the cell viability. Both the CPT-loaded copolymers at their highest concentration (0.5 mg/mL) reduced the cell viability to near about 50% (Fig. 9). It is observed that both CPT-loaded poly[CHOL$_{15}$-co-mPEG$_{5,110}$] and poly[CHOL$_3$-co-mPEG$_{23,22}$] micelles showed almost similar in vitro chemotherapeutic activity towards HeLa cells. As a result of the increased aerobic and anaerobic glycolysis by the tumor cells, the intratumor microenvironment is inherently acidic due to accumulation of lactic acid in high amount [62]. Since the cancer cells are more porous than the normal cells, they can uptake PMs quite easily (as evident from cellular uptake study, Fig. 8) and after internalization of the PMs into the cancer cells; they face an acidic microenvironment within the cancer cells. On the other hand if the PMs enter in the cellular compartment through either endocytosis or other pathways, they conjugate with the acidic lysosomal vesicles (membrane-enclosed organelles that contain an array of enzymes capable of breaking down all types of biological polymers—proteins, nucleic acids, carbohydrates, and lipids) [63] and consequently, the degradation of the PMs occur with the concomitant release of the entrapped drug molecules in the lysosomal pH.

## 3. Conclusions

In conclusion, we have designed, synthesized, and performed molecular characterization of two novel amphiphilic copolymers poly[CHOL$_{15}$-co-mPEG$_{5,110}$] and poly[CHOL$_3$-co-mPEG$_{23,22}$] using a biocompatible PEG unit [46–48] and cholesterol, responsible for cellular membrane-related bioprocess [40–44]. Both the polymers are able to form spherical stable micellar structures with diameters of ca. 20 and ca. 65 nm, respectively, in aqueous solution (Fig. 2). The CAC values of both copolymers were found to be very low. The microenvironments of the polymeric micelles (PMs) are very viscous as well as less polar compared to bulk water due to having CHOL like steroidal moiety as hydrophobe. Consequently, both these PEG-based copolymers with only ca. 12% hydrophobe (CHOL) content have very good solubilization capacity for the almost water-insoluble drug CPT [3]. We are able to solubilize CPT in 0.1% polymer at a concentration 30–40 times higher than its aqueous solubility at room temperature and this solubilization capacity is also greater than our previously made fatty acid containing PEG based polymers [39]. However, longer mPEG chain in poly[CHOL$_3$-co-mPEG$_{23,22}$] was observed to reduce drug-loading capacity of the PMs. The substantial increase of drug-loading capacity will minimize the use of inactive materials and thus will reduce systemic toxicity. Due to very low hydrophobe content, the cloud point temperatures of the copolymers are much above 310 K which means the PMs are structurally stable at the physiological temperature [55,56]. It has been demonstrated that these nanocarriers can release the encapsulated drug upon decrease of the pH below 7 (Fig. 4). All these properties make them very good candidates for intravenous delivery system for cancer chemotherapy. In vitro evaluation study also revealed that these copolymers are sufficiently biocompatible in the permissible concentration range (Fig. 7 and Fig. S11) and their biocompatibility is also higher than
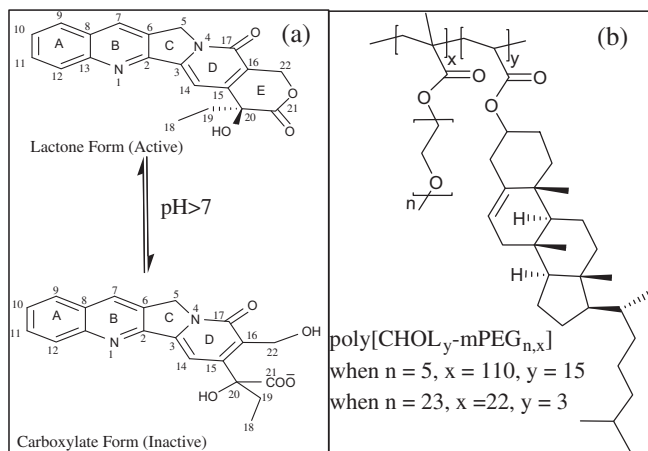


**Chart 1.** Chemical structures of (a) the lactone ring-closed and ring-opened forms of CPT, and (b) poly[CHOL$_y$-co-mPEG$_{n,x}$] copolymers.

the fatty acid containing polymers in the same concentration range [39]. It is interesting to note that while normal (L929) cell membrane is not so much permeable to these polymers, they are easily taken up by the cancer cells (MCF and HeLa) into the cellular compartment (Fig. 8). In vitro activity study of the CPT-loaded PMs of the copolymers on HeLa cells confirmed them to be novel promising nanomedicine for cancer chemotherapy (Fig. 9). Despite difference in molecular weights, hydrodynamic sizes and mPEG chain lengths, CPT-loaded PMs of both poly[CHOL15-co-mPEG5,110] and poly[CHOL3-co-mPEG23,22] copolymers showed similar in vitro chemotherapeutic activity towards HeLa cells.

# 4. Experimental section

## 4.1. Reagents

Methoxy poly(ethylene glycol) methacrylate (mPEG$_n$) of M$_n$ equal to 300 (where $n$ = 5) and 1100 (where $n$ = 23), cholesterol, chloroform-d, and 3-(4,5-dimethlthiazol-2-yl)-2,5-diphenyl-tetrazolium bromide (MTT) were purchased from Sigma–Aldrich (Bangalore, India) and were used without further purification. S-(+)-camptothecin (CPT) (Tokyo Chemical Industry, Japan) was obtained as a gift. Acryloyl chloride was purchased from MERCK, Germany. Radical initiator, 2,2′-azobis-(isobutyronitrile) (AIBN), was purchased from Sigma–Aldrich (Bangalore, India) and was further recrystallized from acetone before use. Fluorescent probes coumarin 153 (C-153), pyrene (Py), and 1,6-diphenyl-1,3,5-hexatriene (DPH) were purchased from Sigma–Aldrich (Bangalore, India) and was recrystallized from ethanol (EtOH) before use. Solvents like methanol (MeOH), dimethyl formamide (DMF), tetrahydrofuran (THF), ethyl acetate, petroleum ether, dichloromethane (DCM) were purchased from Merck and were purified and distilled before use. Milli Q (18.2 M$\Omega$ cm) water was obtained from Millipore water purifier.

## 4.2. Instruments

Melting point was determined with an Instind (Kolkata) melting point apparatus in open capillaries. The pH of the various solutions was measured by using a digital pH meter (pH 5652, EC India Ltd., Kolkata). The UV–vis spectra were recorded on a Shimadzu (Model UV-2450) spectrophotometer. Molecular weight and polydispersity ($D$) of the copolymers were determined by gel permeation chromatography (GPC) using a Viscotek (VE 3580 RI Detecto & VE 1122 Solvent Delivery System) GPC system. Polystyrene (Viscotek, PolyCAL™) having molecular weight in the range 400–3 × 10$^5$ were used as standard. THF (HPLC grade) was used as an eluent at a flow rate of 1 ml/min at 298 K. IR spectra of the compounds were recorded on a Perkin Elmer IR spectrometer (Model 883). The $^1$H and $^{13}$C NMR spectra were recorded on a Bruker Avance 400 spectrometer operated at 400 MHz using TMS as internal reference standard.

## 4.3. Surface tension measurement

Surface tension ($\gamma$) of the aqueous copolymer solution was measured with a surface tensiometer (model 3S, GBX, France) at 298 K using Du Nuöy ring detachment method. The platinum ring was washed with EtOH–HCl solution and was burnt in the oxidizing flame immediately before use. The surface tension of distilled water was measured every time before the experiment started with polymer solutions. Since the polymers were neutral, the stock of polymer solution was made in Milli-Q water only. For every measurement at different concentrations, a definite amount of aliquot from stock of polymer solution was added to a fixed amount

of water in a Teflon beaker and stirred for 10–15 min for equilibration. Surface tension ($\gamma$) for each polymer concentration was measured in triplicate and an average surface tension value was taken.

## 4.4. Fluorescence measurements

Steady-state fluorescence spectra of different fluorescent probes (Py and DPH) were measured with a SPEX Fluorolog-3 spectrophotometer (450 WATT ILLUMINATOR, Model: FL-1039/40, HORIBA JOBIN YVON, EDISON, NJ, USA). An aliquot of Py stock solution (1.0 × 10$^{-3}$ M) in MeOH was added into 5-mL volumetric flasks and the methanol was evaporated by a stream of N$_2$ gas. Then polymer solutions in Milli-Q water of different concentrations were added to the above volumetric flasks, making the final concentration of Py or DPH (1.0 × 10$^{-6}$ M). The mixtures were shaken vigorously for 30 min at room temperature and were kept in a dark place for 12 h. The samples containing Py were excited at 343 nm, and the emission spectra were recorded in the range of 350–600 nm. The excitation and emission slit widths were 10 and 2 nm, respectively. Solutions containing DPH were excited at 350 nm and emission intensity was recorded in the wavelength range 360–550 nm. Steady-state fluorescence anisotropy ($r$) measurements using DPH were performed with a Perkin Elmer LS-55 spectrophotometer equipped with a thermostated cell holder and filter polariser/analyzer assembly that used the L-format configuration. The DPH fluorescence was monitored at 450 nm and each anisotropy measurement was repeated at least six times and an average $r$-value was recorded. The temperature of the samples was controlled by the water jacketed magnetically stirred cell holder in the spectrometer connected to a Thermo Neslab RTE-7 circulating water bath that enabled the temperature control within ±0.1 °C. Temperature-dependent fluorescence measurements were performed in the range of 293–343 K with an increment of 5 K. Before every measurement, the solution was equilibrated at the desired temperature for at least 10 min.

Fluorescence lifetimes of the DPH probe in copolymer solutions were obtained from time-resolved intensity decays measured with a spectrometer (Optical Building Blocks Corporation, Easylife) using time-correlated single-photon counting (TCSPC) technique. A nanosecond diode laser at $\lambda$ = 370 nm was used as the light source for excitation. The fluorescence decay kinetics of DPH was recorded at the emission wavelength of 450 nm. The $\eta_m$ value was calculated from the fluorescence lifetime and anisotropy data as described elsewhere [53,54].

## 4.5. Dynamic light scattering (DLS)

The hydrodynamic size of polymers in aqueous media was monitored by DLS technique Malvern Nano ZS instrument employing a 4 mW He–Ne laser ($\lambda$ = 632.8 nm). All the scattering photons were collected at a 173° scattering angle. The temperature was set to 298 K or 310 K and before every measurement each polymer solution was filtered through 0.45 $\mu$m (Millipore Millex syringe filter) filter paper. It is the instrumental software which processed scattering intensity data to give the hydrodynamic diameter ($d_h$) and the size distribution(s) for each sample. The corresponding hydrodynamic radius or diameter of the PMs was actually calculated using cumulant analysis and Stokes–Einstein equation. The DLS measurements for each sample was repeated three times.

## 4.6. Transmission electron microscopy (TEM)

Transmission electron micrographs with high resolution (JEOL-JEM 2100, Japan) and without high resolution (TECNAI G$^2$-20S TWIN, Japan) were taken for the polymers at different concentrations above their corresponding CAC values, operating at an

accelerating voltage of 200 kV and 120 kV, respectively, at room temperature. For every sample, 5 μL of the polymer solution in water was placed on a carbon-coated copper grid (400 mesh size), excess water was blotted off by use of a filter paper, and was kept in desiccators overnight for drying before taking the micrographs. Each measurement was repeated at least twice to check reproducibility and thus eliminate the possibility of any artifacts.

### 4.7. Solubilization of hydrophobic drugs

Solubilization of CPT was carried out by solvent evaporation method [64]. Same amount of the drug with a required amount of polymer was dissolved in 2 mL of $CHCl_3$ and sonicated for 5 min. Then the $CHCl_3$ solution was added drop wise into 10 mL of MilliQ water. The mixture was stirred in a round bottomed flask for 4–5 h to completely remove the $CHCl_3$. The resulting mixture was stirred in a dark place at room temperature for another 24 h with the stopper into ensure the solubilization equilibrium. The supernatant solution was then filtered using Millipore Millex filter (0.45 μm pore diameter) to remove the insoluble drug. An aliquot was taken from the filtrate and diluted with methanol to measure the absorbance value at 360 nm by a UV–vis spectrophotometer (Shimadzu, Model UV-2450). The copolymer solution at the same dilution was used as a blank. A previously recorded calibration curve was used to calculate the drug concentration.

### 4.8. Hemolytic assay

Hemolytic assay for the polymers was performed using the standard protocol [65]. The polymers were dissolved in PBS (pH 7.4). RBCs' were harvested from human blood by centrifugation at 3000 rpm for 10 min at room temperature. The collected RBC was washed 4 times with 150 mM NaCl solution followed by suspended in PBS to a final cell concentration of $5 \times 10^8$ RBC/mL. The desired amount of polymer was added into 200 μL of the above RBC suspension and the final volume was made up to 1 mL with PBS. In case of positive and negative control, RBC cells were suspended in triton X-100 (1%, w/v) and PBS, respectively. All the samples were then incubated for 60 min at 310 K with an intermittent mixing by inversion of the microcentrifuge tubes. After centrifugation at 12,000 rpm for 5 min, the supernatants were taken and their absorbance values at 541 nm were measured in ELISA reader (Biorad, USA) using PBS as the blank. Each experiment was performed in triplicate.

### 4.9. Cell viability assay

The cytotoxicity is normally measured by cell viability assay which was performed following standard protocol with some modifications [65]. MCF7 cells and HeLa cell were cultured in DMEM (Dulbecco's Modified Eagle's Medium) supplemented with 10% fetal bovine serum (FBS), antibiotics solution containing penicillin (100 units/mL), streptomycin (0.1 mg/mL), and amphotericin B (0.25 μg/mL). The cells were maintained at 310 K in T-25 flasks in a humidified incubator (5% $CO_2$) with a feeding cycle of 48 h. The confluent cell monolayer was trypsinized (0.25% Trypsin + 0.1% EDTA) and cells were harvested by centrifugation.

The copolymers were dissolved in incomplete DMEM medium (pH 7.4) and filtered through 0.2 μm polycarbonate filter. Cell suspensions were seeded at $3 \times 10^3$ cells/well in 100 μL of complete DMEM in a 96-well plate. The cells were allowed to adhere and were grown for 24 h at 310 K in an incubator. The medium was aspirated and replaced with 100 μL of fresh medium containing control and polymers with the desired concentrations. After 24 h (MCF7) or 12 h (HeLa) of incubation with the polymers, the medium was removed and cells were washed thrice with sterile phosphate buffer saline (PBS). Cell viability was performed using a conventional MTT dye reduction assay. A 100 μL of MTT reagent (0.5 g/L in PBS) was added to each well and incubated for 3 h. MTT reagent mixture was gently removed and 200 μL of DMSO was added into each well. The developed formazan dye was measured spectrophotometrically at 540 nm. This experiment was performed in triplicate. The cytotoxic effects of the polymers were expressed as percentage of cell viability with respect to the untreated control cells. The following formula was used to calculate cell viability:

Cell viability (%) = (Mean of Absorbance value of treated cells/ Mean of Absorbance value of untreated control cells) × 100.

### 4.10. Cellular uptake

Confocal microscopy was used for the study of cellular uptake [66] of these polymers using C153 as fluorescent probe (excitation at 422 nm and emission at 510 nm). An aliquot of the C153 stock solution ($1.0 \times 10^{-3}$ M) in methanol was added into 5-mL volumetric flasks and the methanol was evaporated by a stream of $N_2$ gas. Then polymer solutions in PBS (pH 7.4) of different concentrations were added into the above volumetric flasks, making the final concentration of C153 $1.0 \times 10^{-6}$ M. After 12 h, each sample was dialyzed against PBS solution (pH 7.4) for 2–3 h to remove the excess dye which was not solubilized in the hydrophobic core of the polymer. Both the MCF7 (breast cancer cells) and L929 (normal fibroblast cells) cells of mid log phase growth were seeded in a 24 well flat bottom plate at a concentration of $3 \times 10^3$/well and were grown for 24 h at 310 K in a $CO_2$ environment. The media was then aspirated and was replaced with PBS containing various concentrations of polymers followed by 3 h of incubation at 310 K. After this treatment, the PBS was aspirated; wells were washed thrice with PBS and were finally suspended in 200 μL of PBS. Imaging studies were done in Olympus confocal microscope (FV1000, Olympus).

### Author contributions

All authors have given approval to the final version of the manuscript.

### Acknowledgments

### Appendix A. Supplementary material

Supplementary data associated with this article can be found, in the online version, at http://dx.doi.org/10.1016/j.jcis.2014.05.068.

### References

[1] J. Fassberg, V.J. Stella, J. Pharm. Sci. 81 (1992) 676–684.
[2] Z. Mi, T.G. Burke, Biochemistry 33 (1994) 10325–10336.
[3] N.J. Rahier, B.M. Eisenhauer, R. Gao, S.H. Jones, S.M. Hecht, Org. Lett. 6 (2004) 321–324.
[4] J.W. Singer, R. Bhatt, J. Tulinsky, K.R. Buhler, E. Heasley, P. Klein, P. de Vries, J. Controlled Release 74 (2001) 243–247.
[5] R.B. Greenwald, H. Zhao, J. Xia, Bioorg. Med. Chem. 11 (2003) 2635–2639.
[6] A.B. Fleming, K. Haverstick, W.M. Saltzman, Bioconjugate Chem. 15 (2004) 1364–1375.
[7] Z. Cao, N. Harris, A. Kozielski, D. Vardeman, J.S. Stehlin, B. Giovanella, J. Med. Chem. 41 (1998) 31–37.

[8] H. Zhao, C. Lee, P. Sai, Y.H. Choe, M. Boro, A. Pendri, R.B. Greenwald, J. Org. Chem. 65 (2000) 4601–4606.
[9] R.B. Greenwald, A. Pendri, C. Conover, C. Gilbert, R. Yang, J. Xia, J. Med. Chem. 39 (1996) 1938–1940.
[10] V.R. Caiolfa, M. Zamai, A. Fiorino, E. Frigerio, C. Pelliz-zoni, R. d'Argy, A. Suarato, J. Controlled Release 65 (2000) 105–119.
[11] R. Bhatt, P. de Vries, J. Tulinsky, G. Bellamy, B. Baker, J.W. Singer, P. Klein, J. Med. Chem. 46 (2003) 190–193.
[12] A.V. Yurkovetskiy, A. Hiller, S. Syed, M. Yin, X.M. Lu, A.J. Fischman, M.I. Papisov, Mol. Pharm. 1 (2004) 375–382.
[13] H. Maeda, Adv. Enzyme Regul. 41 (2001) 189–207.
[14] W. Zhang, J. Huang, N. Fan, J. Yu, Y. Liu, S. Liu, Y. Li, Colloids Surf., B 81 (2010) 297–303.
[15] N. Fan, K. Duan, C. Wang, S. Liu, S. Luo, J. Yu, D. Wang, Colloids Surf., B 75 (2010) 543–549.
[16] Y. Shen, E. Jin, B. Zhang, C.J. Murphy, M. Sui, J. Zhao, W.J. Murdoch, J. Am. Chem. Soc. 132 (2010) 4259–4265.
[17] B.S. Lee, A.K. Nalla, I.R. Stock, T.C. Shear, K.L. Black, J.S. Yu, Bioorg. Med. Chem. Lett. 20 (2010) 5262–5268.
[18] X.Q. Li, H.Y. Wen, H.Q. Dong, W.M. Xue, G.M. Pauletti, X.J. Cai, Y.Y. Li, Chem. Commun. 47 (2011) 8647–8649.
[19] X. Liu, B.C. Lynn, J. Zhang, L. Song, D. Bom, W. Du, T.G. Burke, J. Am. Chem. Soc. 124 (2002) 7650–7651.
[20] W. Tong, L. Wang, M.J. D'Souza, Drug Dev. Ind. Pharm. 29 (2003) 745–756.
[21] V. Kumar, J. Kang, R.J. Hohl, Pharm. Dev. Technol. 6 (2001) 459–467.
[22] K.M. Tyner, S.R. Schiffman, E.P. Giannelis, J. Controlled Release 95 (2004) 501–514.
[23] Z.R. Huang, Acta Pharmacol. Sin. 29 (2008) 1094–1102.
[24] O.M. Koo, I. Rubinstein, H. Onyuksel, Nanomedicine (N. Y., NY, U.S.) 1 (2005) 77–84.
[25] V.J. Venditto, K. Allred, C.D. Allred, E.E. Simanek, Chem. Commun. 37 (2009) 5541–5542.
[26] S. Yang, J. Zhu, Y. Lu, B. Liang, C. Yang, Pharm. Res. 16 (1999) 751–757.
[27] J.Y. Fang, C.F. Hung, S.C. Hua, T.L. Hwang, Ultrasonics 49 (2009) 39–46.
[28] M. Yokoyama, S. Fukusima, R. Uehara, K. Okamoto, K. Kataoka, Y. Sakurai, T. Okano, J. Controlled Release 50 (1998) 79–92.
[29] T.Y. Kim, D.W. Kim, J.Y. Chung, S.G. Shin, S.C. Kim, D.S. Heo, N.K. Kim, Y.J. Bang, Clin. Cancer Res. 10 (2004) 3708–3716.
[30] A.L.Z. Lee, S. Venkataraman, S.B.M. Sirat, S. Gao, J.L. Hedrick, Y.Y. Yang, Biomaterials 33 (2012) 1921–1928.
[31] N. Nishiyama, S. Okazaki, H. Cabral, M. Miyamoto, Y. Kato, Y. Sugiyama, K. Nishio, Y. Matsumura, K. Kataoka, Cancer Res. 63 (2003) 8977–8983.
[32] Y. Li, G.S. Kwon, Pharm. Res. 17 (2000) 607–611.
[33] (a) Y. Wang, H. Wang, G. Liu, X. Liu, Q. Jin, J. Ji, Macromol. Biosci. 13 (2013) 1084–1091;
(b) W. Cheng, J.N. Kumar, Y. Zhang, Y. Liu, pH-and redox-responsive poly(ethylene glycol) and cholesterol-conjugated poly(amido amine)s based micelles for controlled drug delivery. Macromol. Biosci. <http://dx.doi.org/10.1002/mabi.201300339> (in press).
[34] K. Greish, J. Fang, T. Inutsuka, A. Nagamitsu, H. Maeda, Clin. Pharmacokinet. 42 (2003) 1089–1105.
[35] K. Kawano, M. Watanabe, T. Yamamoto, M. Yokoyama, P. Opanasopit, T. Okano, Y. Maitaini, J. Controlled Release 112 (2006) 329–332.
[36] P. Opanasopit, M. Yokoyama, M. Watanabe, K. Kawano, Y. Maitaini, T. Okano, Pharm. Res. 21 (2004) 2001–2008.
[37] M. Watanabe, K. Kawano, M. Yokoyama, P. Opanasopit, T. Okano, Y. Maitaini, Int. J. Pharm. 308 (2006) 183–189.
[38] (a) P. Dutta, J. Dey, V. Perumal, M. Mandal, Int. J. Pharm. 407 (2011) 207–216;
(b) P. Dutta, J. Dey, Int. J. Pharm. 421 (2011) 353–363.
[39] P. Laskar, B. Saha, S. Ghosh, J. Dey, RSC Adv. (2014) (in preparation).
[40] P.L. Yeagle, Biochimie 73 (1991) 1303–1310.
[41] P.L. Yeagle, Biochim. Biophys. Acta 822 (1985) 267–287.
[42] J.P. Incardona, S. Eaton, Curr. Opin. Cell Biol. 12 (2000) 193–203.
[43] F.R. Maxfield, I. Tabas, Nature 438 (2005) 612–621.
[44] K. Simons, E. Ikonen, Science 290 (2000) 1721–1726.
[45] (a) K. Park, K. Kim, I.C. Kwon, S.K. Kim, S. Lee, D.Y. Lee, Y. Byun, Langmuir 20 (2004) 11726–11731;
(b) K. Akiyoshi, S. Deguchi, N. Moriguchi, S. Yamaguchi, J. Sunamoto, Macromolecules 26 (1993) 3062–3068.
[46] P. Aggarwal, J.B. Hall, C.B. McLeland, M.A. Dobrovolskaia, S.E. McNeil, Adv. Drug Delivery Rev. 61 (2009) 428–437.
[47] G. Liu, S. Ma, S. Li, R. Cheng, F. Meng, H. Liu, et al., Biomaterials 31 (2010) 7575–7585.
[48] R. Namsung, K. Singha, M.K. Yu, S. Jon, Y.S. Kim, Y. Ahn, et al., Biomaterials 31 (2010) 4204–4213.
[49] S.N. Patil, F. Liu, J. Org. Chem. 73 (2008) 4476–4483.
[50] A. Nakajima, J. Mol. Spectrosc. 61 (1976) 467–469.
[51] K. Kalyanasundaram, J.K. Thomas, J. Am. Chem. Soc. 99 (1977) 2039–2044.
[52] M. Shinitzky, Physical Methods on Biological Membranes and their Model Systems, Plenum Publishing Corp., New York, 1984. p. 237.
[53] S. Roy, A. Mohanty, J. Dey, Chem. Phys. Lett. 414 (2005) 23–27.
[54] P. Debye, Polar Molecules, Dover, New York, 1929.
[55] S.V. Aathimanikandan, E.N. Savariar, S. Thayumanavan, J. Am. Chem. Soc. 127 (2005) 14922–14929.
[56] J. Zhou, F. Ke, Y.-Y. Tong, Z.-C. Li, D. Liang, Soft Matter 7 (2011) 9956–9961.
[57] R.B. Greenwald, Y.H. Choe, J. McGuire, C.D. Conover, Adv. Drug Delivery Rev. 55 (2003) 217–250.
[58] D. Yu, P. Peng, S.S. Dharap, Y. Wang, M. Mehlig, P. Chandna, H. Zhao, D. Filpula, K. Yang, V. Borowski, G. Borchard, Z. Zhang, T. Minko, J. Controlled Release 110 (2005) 90–102.
[59] J. Dey, I.M. Warner, J. Lumin. 71 (1997) 105–114.
[60] (a) Z. Guo, S. Meng, W. Zhong, Q. Du, L.L. Chou, Appl. Surf. Sci. 255 (2009) 6771–6780;
(b) J. Hoffmann, J. Groll, J. Heuts, H. Rong, D. Klee, G. Ziemer, M. Moeller, H.P. Wendel, J. Biomater. Sci., Polym. Ed. 17 (2006) 985–996.
[61] S. Chen, X.Z. Zhang, S.X. Cheng, R.X. Zhuo, Z.W. Gu, Biomacromolecules 9 (2008) 2578–2585.
[62] a C.W. Song, R. Griffin, H.J. Park, Influence of tumor pH on therapeutic response, in: Cancer Drug Resistance, Humana Press, 2006, pp. 21–42;
b C.W. Song, J.C. Lyon, Y. Luo, Intra- and extracellular pH in solid tumors: influence on therapeutic response, in: B.V. Teicher (Ed.), Drug Resistance in Oncology, Marcel Dekker, New York, 1993, pp. 25–51.
[63] (a) I. Mellman, R. Fuchs, A. Helenius, Annu. Rev. Biochem. 55 (1986) 663–700;
(b) N. Rapoport, A. Marin, Y. Luo, G.D. Prestwich, M.D. Muniruzzaman, J. Pharm. Sci. 91 (2002) 157–170.
[64] A. Lavasanifar, J. Samuel, G.S. Kwon, J. Controlled Release 77 (2001) 155–160.
[65] M.E. El-Sayed, A.S. Hoffman, P.S. Stayton, J. Controlled Release 101 (2005) 47–58.
[66] A. Sulistio, J. Lowenthal, A. Blencowe, M.N. Bongiovanni, L. Ong, S.L. Gras, G.G. Qiao, Biomacromolecules 12 (2011) 3469–3477.